Article

Immunity

The Chemokine Receptor CX3CR1 Defines Three Antigen-Experienced CD8 T Cell Subsets with Distinct Roles in Immune Surveillance and Homeostasis

Graphical Abstract

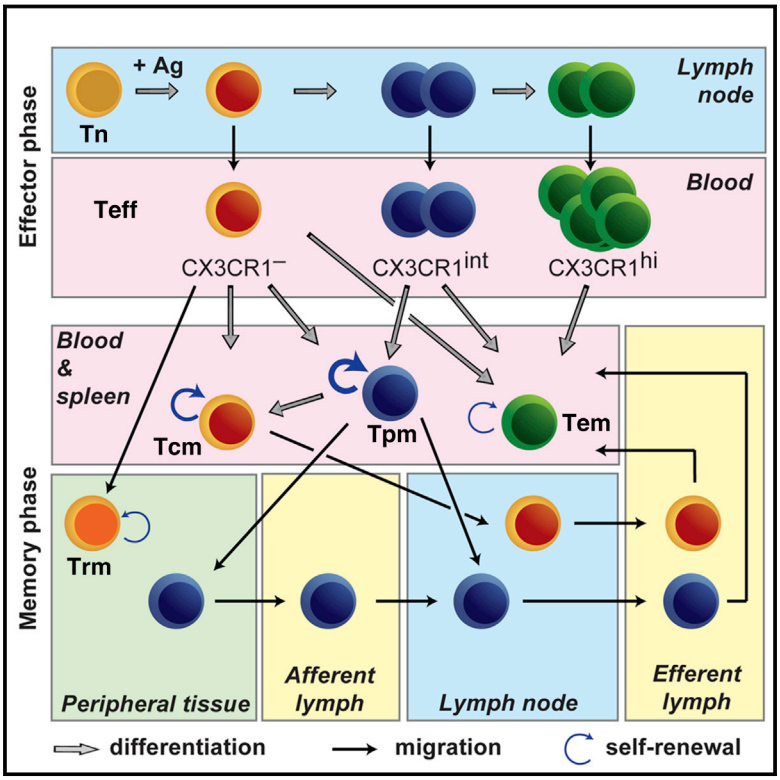

Authors

Carmen Gerlach, E. Ashley Moseman, Scott M. Loughhead, ..., Rohit Garg, Juan C. de la Torre, Ulrich H. von Andrian

Correspondence

uva@hms.harvard.edu

In Brief

Gerlach et al. (2016) demonstrate that CX3CR1 identifies three distinct CD8$^+$ effector and memory T cell (Tmem) subsets. CX3CR1 correlated with the degree of effector differentiation. Surprisingly, a newly identified CX3CR1^{int} Tmem population, not effector memory cells (CX3CR1^{hi}), was the predominant subset that surveyed non-lymphoid tissues.

Highlights

- CX3CR1 correlates with the degree of effector CD8$^+$ T cell differentiation
- CX3CR1 delineates three Tmem populations with distinct homeostatic properties
- Effector memory T cells are largely excluded from peripheral tissues
- CX3CR1^{int} cells are the predominant Tmem subset surveying peripheral tissues

Gerlach et al., 2016, Immunity *45*, 1270–1284
December 20, 2016
http://dx.doi.org/10.1016/j.immuni.2016.10.018

CellPress

CellPress

Immunity
Article

The Chemokine Receptor CX3CR1 Defines Three Antigen-Experienced CD8 T Cell Subsets with Distinct Roles in Immune Surveillance and Homeostasis

Carmen Gerlach,[1,5] E. Ashley Moseman,[1,4,5] Scott M. Loughhead,[1,5] David Alvarez,[1] Anthonie J. Zwijnenburg,[1] Lisette Waanders,[1] Rohit Garg,[1] Juan C. de la Torre,[2] and Ulrich H. von Andrian[1,3,6,*]

[1]Department of Microbiology and Immunobiology and HMS Center for Immune Imaging, Harvard Medical School, Boston, MA 02115, USA
[2]Department of Immunology and Microbial Science, The Scripps Research Institute, La Jolla, CA 92037, USA
[3]The Ragon Institute of MGH, MIT and Harvard, Cambridge, MA 02139, USA
[4]Present address: National Institute of Neurological Disorders and Stroke, National Institutes of Health, Bethesda, MD 20892, USA
[5]Co-first author
[6]Lead Contact
*Correspondence: uva@hms.harvard.edu
http://dx.doi.org/10.1016/j.immuni.2016.10.018

SUMMARY

Infections induce pathogen-specific T cell differentiation into diverse effectors (Teff) that give rise to memory (Tmem) subsets. The cell-fate decisions and lineage relationships that underlie these transitions are poorly understood. Here, we found that the chemokine receptor CX3CR1 identifies three distinct CD8$^+$ Teff and Tmem subsets. Classical central (Tcm) and effector memory (Tem) cells and their corresponding Teff precursors were CX3CR1$^-$ and CX3CR1^{high}, respectively. Viral infection also induced a numerically stable CX3CR1^{int} subset that represented ~15% of blood-borne Tmem cells. CX3CR1^{int} Tmem cells underwent more frequent homeostatic divisions than other Tmem subsets and not only self-renewed, but also contributed to the expanding CX3CR1$^-$ Tcm pool. Both Tcm and CX3CR1^{int} cells homed to lymph nodes, but CX3CR1^{int} cells, and not Tem cells, predominantly surveyed peripheral tissues. As CX3CR1^{int} Tmem cells present unique phenotypic, homeostatic, and migratory properties, we designate this subset peripheral memory (tpm) cells and propose that tpm cells are chiefly responsible for the global surveillance of non-lymphoid tissues.

INTRODUCTION

When naive CD8$^+$ T cells (Tn) encounter an infection, activation by cognate antigen (Ag) causes them to proliferate and to give rise to T effector (Teff) cells that eradicate the pathogen. Eventually, most Teff cells are eliminated, but a small fraction persists as long-lived memory (Tmem) cells (Williams and Bevan, 2007).

Both Teff and Tmem cells are composed of distinct subsets (Jameson and Masopust, 2009; Mueller et al., 2013). At the Teff stage, differential expression of KLRG1 (killer cell lectin-like receptor G1) and CD127 is commonly used to identify differentiation states that differ in their propensity to form memory. The two major known Tmem populations in blood and spleen are central memory (Tcm) and effector memory (Tem) cells, which are traditionally defined by differential expression of the lymph node (LN) homing receptors CD62L and CCR7 (Marzo et al., 2005; Sallusto et al., 1999; Wherry et al., 2003). Tcm cells have a higher proliferative capacity and are thought to provide superior protection against reinfection than Tem cells, at least in some settings. Tem cells, in contrast, are more cytotoxic than Tcm cells. Because naive (Tn) and Tcm cells (but not Tem cells) express CCR7 and CD62L, they can home to LNs via high endothelial venules (HEV) and survey LNs for cognate Ag (von Andrian and Mempel, 2003). After a few hours to days, these migratory T cells egress from LNs and return to the blood via the efferent lymphatics and thoracic duct (TD) (Gowans and Knight, 1964). Some Tmem cells are also present in afferent lymphatics that drain interstitial fluid from peripheral tissues into LNs (Mackay et al., 1990). Because Tem cells cannot home directly to LNs via HEV, it had been postulated that circulating Tem cells continuously survey non-lymphoid tissues and return to the blood via the draining lymph conduits (Sallusto et al., 1999). To date, this widely held idea has not been tested by rigorous experiments.

A third Tmem subset—tissue-resident memory cells (Trm)—was recently identified (Mueller et al., 2013). This tissue-confined, non-migratory Tmem population is derived from Teff cells that seed non-lymphoid tissues early after infection (Mackay et al., 2013; Masopust et al., 2010; Stary et al., 2015). It has also been suggested that Trm cells might be progeny of Tem cells (Jiang et al., 2012). In contrast, whether Tem and Tcm cells have distinct precursors within the Teff population is unclear, and the rules that determine the differentiation of these Tmem subsets remain largely elusive. These uncertainties are due, at least in part, to the lack of phenotypic markers that can link Teff differentiation states to specific Tmem subsets. Consequently, the relationship between Tem, Tcm, and Trm cells has been a subject of debate (Marzo et al., 2005; Wherry et al., 2003).

Aside from the Tcm/Tem paradigm, Tmem cells have also been sub-divided based on differential expression of phenotypic markers, including CD27 (Hamann et al., 1997), CD127 (Kaech et al., 2003), KLRG1, CD43 (1B11) (Hikono et al., 2007; Joshi

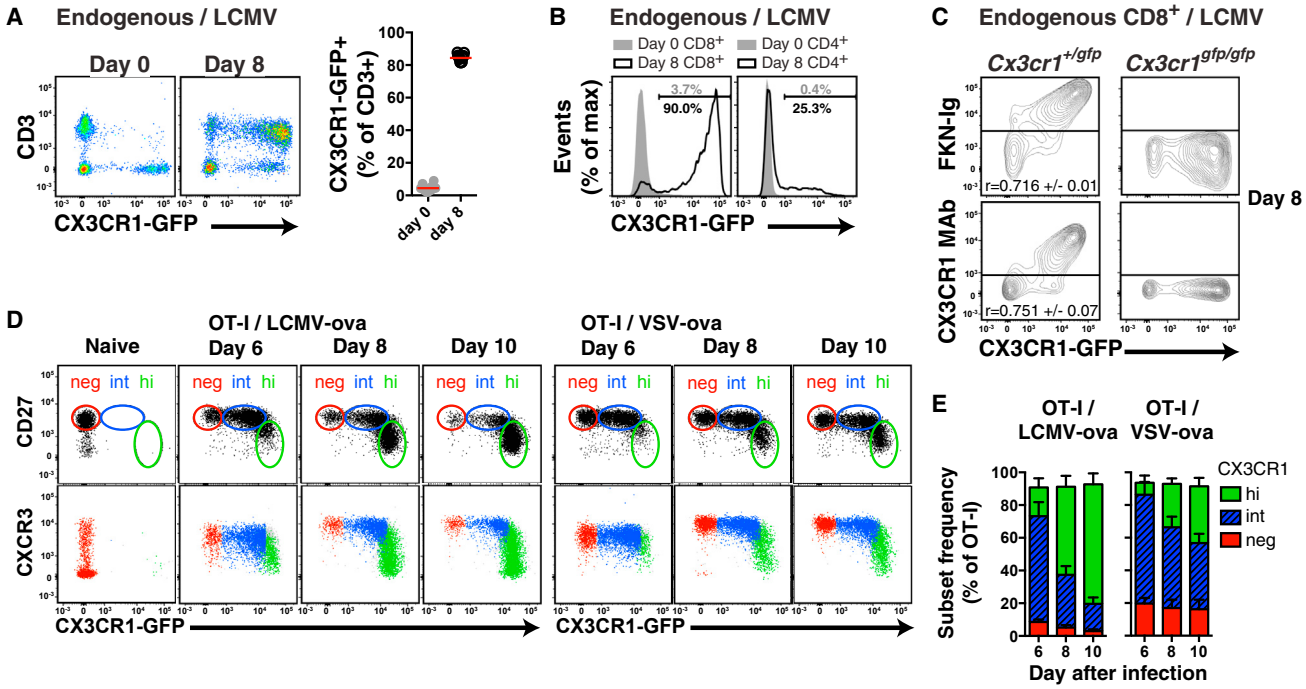

Figure 1. CX3CR1 Expression Levels Identify Three Populations of Pathogen-Specific CD8$^+$ Teff Cells

(A) FACS analysis of CX3CR1-GFP induction by LCMV infection on PBMC (left: representative experiment; right: means of 3 experiments, n = 3–5 mice/each) and (B) after gating on CD3$^+$CD8$^+$ or CD3$^+$CD4$^+$.

(C) Staining of CD8 T cells by fractalkine fused to human IgG1 F_c (FKN-Ig) or CX3CR1 mAb. r, mean Pearson correlation ± SD.

(D and E) Naive *Cx3cr1*$^{+/gfp}$ CD45.1$^+$ OT-I cells were transferred into C57BL/6 recipients followed by LCMV-ova or VSV-ova infection. (D) Gating strategy to identify Teff subsets. (E) Mean + SD n = 2 experiments. All FACS plots are composite plots as described in Figure S1A. See also Figures S1–S3.

et al., 2007; Olson et al., 2013; Sarkar et al., 2008; Voehringer et al., 2001), and, recently, CX3CR1 (Böttcher et al., 2015). For example, KLRG1$^-$CD27$^+$ Tmem cells mount more potent recall responses than KLRG1$^+$ Tmem cells (Hikono et al., 2007). Similarly, CX3CR1$^+$ Tmem cells exhibit robust cytotoxicity, while CX3CR1$^-$ Tmem cells are largely non-cytotoxic and possess greater proliferative capacity (Böttcher et al., 2015).

The present study was prompted by the observation that in response to lymphocytic choriomeningitis virus Armstrong (LCMV) infection, the CX3CR1$^+$ CD8$^+$ T cell subset could be further subdivided into two distinct populations that express CX3CR1 at intermediate or high levels. Thus, we investigated the properties of CX3CR1$^-$, CX3CR1^{int}, and CX3CR1^{hi} Teff and Tmem cells and their relationship to the classical Tcm, Tem, and Trm subsets that arise in response to systemic infections.

We demonstrate that CX3CR1^{int} Tmem cells represent a distinct subset that differs from Tcm (CX3CR1$^-$), Tem (CX3CR1^{hi}), and Trm (CX3CR1$^{-/low}$) cells in its phenotypic, migratory, and homeostatic properties. CX3CR1^{int} Tmem cells possessed the highest steady-state self-renewal capacity of all Tmem subsets and were the predominant Tmem subset surveying peripheral tissues.

RESULTS

Viral Infection Induces CX3CR1 on Virus-Specific CD8$^+$ Teff Cells

To monitor CX3CR1 expression during viral infection, we intravenously (i.v.) injected LCMV into *Cx3cr1*$^{+/gfp}$ reporter mice in which green fluorescent protein (GFP) was "knocked in" the *Cx3cr1* locus (Jung et al., 2000). Consistent with previous studies (Böttcher et al., 2015; Jung et al., 2000), uninfected *Cx3cr1*$^{+/gfp}$ mice were devoid of GFP$^+$ T cells. However, acute LCMV infection induced GFP expression in > 80% of *Cx3cr1*$^{+/gfp}$ T cells (Figure 1A and S1A). This reflected primarily CD8$^+$ T cells, as only a few CD4$^+$ T cells moderately upregulated GFP (Figure 1B and S1B–S1F). GFP levels on *Cx3cr1*$^{+/gfp}$ CD8$^+$ T cells correlated with binding of fractalkine and anti-CX3CR1 monoclonal antibody (mAb; Figure 1C). Neither reagent stained *Cx3cr1*$^{gfp/gfp}$ (*Cx3cr1* knock-out) cells, indicating that GFP levels on hemizygous T cells specifically reported functional CX3CR1. The frequency and phenotype of GFP$^+$ T cells was similar in infected *Cx3cr1*$^{+/gfp}$ and *Cx3cr1*$^{gfp/gfp}$ mice, suggesting that CX3CR1 itself is not required for Ag recognition or Teff differentiation.

CX3CR1 Expression Levels Distinguish Three Virus-Specific CD8$^+$ Teff Subsets

To address whether CX3CR1 acquisition required Ag recognition, we crossed CD45.1$^+$ *Cx3cr1*$^{+/gfp}$ mice with T cell receptor transgenic (TCR-tg) OT-I or P14 animals, whose CD8$^+$ T cells recognize the SIINFEKL peptide of ovalbumin (OVA) or an immunodominant LCMV epitope, gp_{33-41}, respectively. When both TCR-tg Tn populations were co-transferred into congenic (CD45.2$^+$) C57BL/6 mice, only P14 cells upregulated GFP after LCMV challenge (Figure S2A). By contrast, OVA-expressing LCMV induced CX3CR1 in both TCR-tg populations (Figure S2B). *Cx3cr1*$^{+/gfp}$ OT-I cells also upregulated CX3CR1 when animals

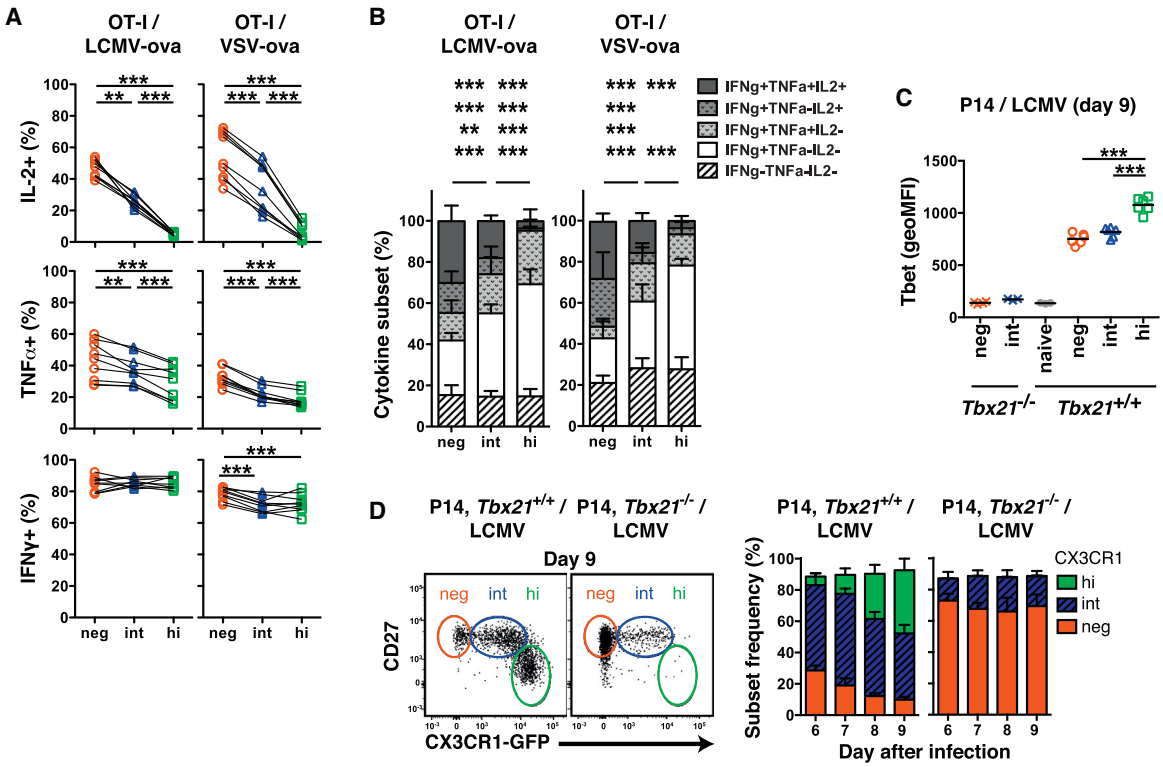

Figure 2. CX3CR1 Is a Differentiation Marker for Pathogen-Specific CD8⁺ Teff Cells

(A and B) Naive *Cx3cr1*$^{+/gfp}$ CD45.1^{+} OT-I cells were transferred into C57BL/6 recipients followed by LCMV-ova or VSV-ova infection. Cytokine expression by splenic Teff subsets (day 10), gated as in Figure 1D (B, mean + SD).

(C) Naive p14 *Cx3cr1*$^{+/gfp}$ CD45.1^{+} [*Tbx21*$^{+/+}$ or *Tbx21*$^{-/-}$] cells were transferred into C57BL/6 followed by LCMV infection and analysis of splenic P14 cells.

(D) Naive p14 *Cx3cr1*$^{+/gfp}$ (*Tbx21*$^{+/+}$ [CD45.1^{+}CD45.2^{-}] or *Tbx21*$^{-/-}$ [CD45.1^{+}CD45.2^{+}]) were co-transferred to C57BL/6 mice followed by LCMV infection. Left shows composite plots of blood-derived P14 T cells; right shows mean + SD.

(A-D) n = 2 experiments pooled. **p < 0.01, ***p < 0.001 by repeated-measures one-way (A), repeated-measures two-way (B) or regular one-way (C) ANOVA with Tukey's (A,C) or Bonferroni (B) multiple comparisons test. See also Figure S3and Figures S4A and S4B.

were infected with other OVA expressing pathogens (Figures S2C–S2E). Thus, CX3CR1 induction on CD8^{+} T cells requires cognate TCR triggering.

Regardless of the pathogen or cognate Ag, CX3CR1 induction followed a typical pattern: starting on day 5, some CD8^{+} T cells expressed intermediate CX3CR1 levels, and expression subsequently intensified. Even at maximal CX3CR1 expression, three subsets were distinguishable: most Teff cells were CX3CR1^{hi}, a few remained CX3CR1^{-}, while others were CX3CR1^{int} (Figures 1D and 1E). All subsets displayed characteristics of recent activation, such as high expression of CD44, the 1B11 glycoform of CD43 and loss of CD62L (Figures S3A and S3B). The chemokine receptor CXCR3, which is largely absent from Tn cells, was upregulated on CX3CR1^{-} and CX3CR1^{int} cells, but was lost from CX3CR1^{hi} cells.

CX3CR1 Correlates with the Degree of Effector Differentiation

Next, we asked whether CX3CR1 levels correspond to the progressive Teff differentiation states that correlate inversely with Tmem generation potential (Gerlach et al., 2011). CX3CR1^{-}, CX3CR1^{int}, and CX3CR1^{hi} CD8^{+} Teff cells expressed distinct differentiation-associated markers, regardless of the pathogen (Figure 1D and S3C–S3F). CX3CR1^{hi} Teff cells were CD27^{-}, CD127^{-}, and mostly KLRG1^{+}, contained the fewest interleukin-2 (IL-2) producing cells (Figure 2A and 2B and S4A and S4B), and expressed ~50% more Tbet than CX3CR1^{-} and CX3CR1^{int} Teff cells (Figure 2C). This phenotype of the CX3CR1^{hi} subset is typical for terminally differentiated Teff cells (Hintzen et al., 1993; Joshi et al., 2007; Kaech et al., 2003; Sarkar et al., 2008; Voehringer et al., 2001).

As Tbet drives CD8^{+} T cells toward terminal differentiation (Joshi et al., 2007), we investigated Tbet's role in the generation of each subset. Following LCMV infection, *Tbx21*$^{-/-}$ P14 T cells remained mostly CX3CR1^{-} (Figure 2D). Whereas CX3CR1^{int} Teff cells were reduced in frequency, CX3CR1^{hi} cells were completely absent, indicating that Tbet is essential to generate CX3CR1^{hi} Teff cells, but not critical for the CX3CR1^{-} and CX3CR1^{int} subsets.

IL-2 producers were more frequent among CX3CR1^{-} than CX3CR1^{int} Teff cells (Figures 2A and S4A and S4B), suggesting that CX3CR1^{-} Teff cells were least differentiated. Also, CX3CR1^{-} Teff cells contained the most polyfunctional cells that produced IL-2, interferon-γ (IFN-γ), and tumor necrosis factor alpha (TNF-α) (Figures 2A and 2B). Together, these findings suggest a sequence of Teff differentiation, whereby the least

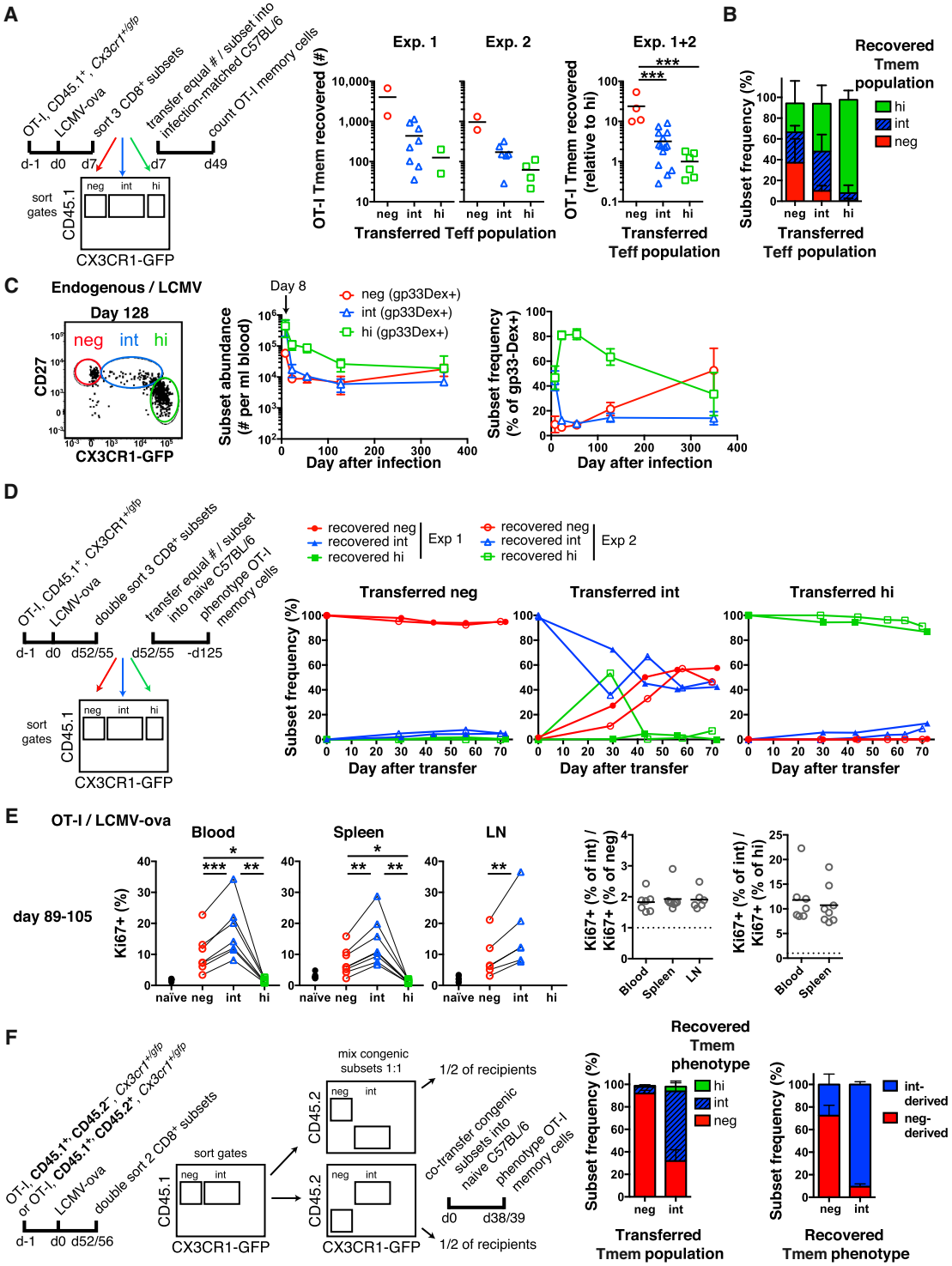

Figure 3. CX3CR1 Expression Levels Identify Three CD8$^+$ Tmem Populations with Distinct Homeostatic Properties

(A) Experimental protocol, absolute and relative numbers, and (B) phenotype of OT-I Tmem cells recovered from spleen and LNs of recipients of sorted Teff subsets. (B) Mean + SD.

(C) *Cx3cr1*$^{+/gfp}$ mice were infected with LCMV. Representative FACS plot and concentration and frequency of gp33-Dextramer$^+$ CD8$^+$ Tmem subsets in blood. Mean ± SD.

(D) Experimental protocol and phenotype of OT-I Tmem cells recovered from spleen and LNs. One mouse per time-point.

(legend continued on next page)

differentiated CX3CR1^{-} cells give rise to CX3CR1^{int} Teff cells, which can progress to the terminally differentiated CX3CR1^{hi} state that is strictly Tbet dependent.

CX3CR1 Expression Levels on Teff Cells Predict Tmem Cell Frequency and Phenotype

Next, we asked whether differential CX3CR1 expression predicts the potential to generate memory. We sorted CX3CR1^{-}, CX3CR1^{int}, and CX3CR1^{hi} OT-I Teff cells and adoptively transferred equal numbers of each subset into separate congenic hosts. The recipients were infection-matched so that the transferred Teff cells encountered the same inflammatory milieu before and after isolation. The three Teff subsets generated markedly different numbers of memory progeny; CX3CR1^{int} Teff cells gave rise to ~3× more Tmem cells than CX3CR1^{hi} Teff cells. CX3CR1^{-} Teff cells generated the largest memory offspring, ranging from 10- to > 50-fold above the Tmem cell number in recipients of CX3CR1^{hi} Teff cells (Figure 3A). The Tmem populations that arose from each transferred Teff subset also differed in phenotype (Figure 3B). Mice that had received CX3CR1^{-} Teff cells contained roughly equal numbers of CX3CR1^{-}, CX3CR1^{int}, and CX3CR1^{hi} Tmem cells on day 49, whereas recipients of CX3CR1^{int} Teff cells generated mainly CX3CR1^{int} and CX3CR1^{hi} Tmem subsets. CX3CR1^{hi} Teff cells gave rise almost exclusively to CX3CR1^{hi} offspring. Thus, CX3CR1 distinguishes not only CD8^{+} Teff subsets with differential capacities to generate early Tmem cells, but CX3CR1 expression on Teff cells also predicts the phenotype of Tmem progeny.

CX3CR1 Expression Delineates Three Tmem Populations with Distinct Homeostatic Properties

In light of the observation that CX3CR1 expression was not restricted to Teff cells, and that many Ag-experienced cells expressed high levels of CX3CR1 after the Teff→Tmem transition, we monitored CX3CR1 expression on gp33-Dextramer^{+} T cells in blood of *Cx3cr1*$^{+/gfp}$ mice during 1 year after LCMV infection (Figure 3C). As with Teff cells, Tmem cells could be subdivided into three subsets based on differential CX3CR1 expression. CX3CR1^{hi} cells were most abundant during the first ~250 days, but diminished over time, while CX3CR1^{-} Tmem cells gradually increased in frequency and became the predominant subset after ~8 months. The frequency of CX3CR1^{int} cells declined initially, reaching ~15% by day 30, and remained stable thereafter.

As reported recently by others (Böttcher et al., 2015), also a subset of human CD8^{+} CD45RO^{+} Tmem cells expressed CX3CR1 (Figure S4C). The frequencies of CX3CR1^{-}, CX3CR1^{int}, and CX3CR1^{hi} Tmem subsets are similar in human and murine blood. Only a fraction of the human CX3CR1^{hi} Tmem lacked CD27, but co-staining with CXCR3 closely paralleled the mouse data.

The gradual change in Tmem subset ratios (Figure 3C) could either reflect differential survival and/or self-renewal of phenotypically stable subsets, or inter-conversion. To test whether CX3CR1^{-}, CX3CR1^{int}, and CX3CR1^{hi} Tmem subsets are phenotypically stable, we adoptively transferred equal numbers of each highly purified subset (double-sorted to > 98% purity) into naive congenic recipients (Figure 3D). CX3CR1^{-} and CX3CR1^{hi} Tmem cells remained phenotypically stable, i.e., > 90% maintained their original CX3CR1 expression levels for > 10 weeks after transfer. In contrast, recipients of CX3CR1^{int} Tmem cells harbored not only CX3CR1^{int} cells, but also generated CX3CR1^{-} cells, which increased in frequency, accounting for ~50% of all recovered memory cells after 2 months. CX3CR1^{int} Tmem cells did not generate CX3CR1^{hi} cells (except in one recipient at a single time point).

The progressive conversion of CX3CR1^{int} Tmem cells into CX3CR1^{-} cells posed a conundrum because neither CX3CR1^{-} nor CX3CR1^{hi} Tmem subsets gave rise to CX3CR1^{int} cells after adoptive transfer, yet the frequency of the latter remained constant for at least 1 year (Figure 3C). Thus, we asked whether CX3CR1^{int} Tmem cells undergo superior homeostatic proliferation. Indeed, a sizeable fraction of CX3CR1^{int} Tmem cells expressed Ki67 at steady-state (Figure 3E), a nuclear protein that is only expressed in cycling cells (Gerdes et al., 1984). Within each animal, dividing CX3CR1^{int} Tmem cells were ~2-fold and ~11-fold more frequent than dividing CX3CR1^{-} or CX3CR1^{hi} Tmem cells, respectively. Consequently, the dynamic changes in Tmem subset frequencies in Figure 3C most likely reflect attrition of the poorly self-renewing CX3CR1^{hi} cells, and vigorous homeostatic division of the CX3CR1^{int} subset that was sufficient to maintain itself at a steady frequency, while simultaneously "feeding" the CX3CR1^{-} Tmem pool.

To further explore how "feeding" of the CX3CR1^{-} Tmem population by CX3CR1^{int} Tmem precursors might contribute to the expansion of the CX3CR1^{-} Tmem pool, we mathematically modeled the CX3CR1^{int}→CX3CR1^{-} conversion dynamics based on Tmem subset frequencies between days 55 and 128 post infection (Figure 3C) and estimates of subset proliferation rates (Figure 3E). Our calculations predict the continuous rate of CX3CR1^{int}→CX3CR1^{-} conversion to be ~0.5% of the entire CX3CR1^{int} Tmem pool, suggesting that during this ~10 weeks long time interval ~31% of CX3CR1^{-} Tcm cells arose from CX3CR1^{int} Tmem cells (Figure S4D; Supplemental Experimental Procedures).

We experimentally tested this prediction by co-transferring congenic CX3CR1^{-} and CX3CR1^{int} Tmem subsets into naive recipients and analyzing the phenotype of each transferred Tmem subset ~40 days later (Figure 3F). In agreement with our result from adoptive transfers of single Tmem populations (Figure 3D), CX3CR1^{-} Tmem cells remained phenotypically stable also in this competitive co-transfer setting, while ~30% of the progeny of co-transferred CX3CR1^{int} Tmem cells became CX3CR1^{-}. Consequently, of all CX3CR1^{-} Tmem cells that were recovered on day ~40 after transfer ~one third was derived from CX3CR1^{int} cells. These results closely matched our (somewhat conservative)

(E) Frequency of Ki67^{+} cells among naive (CD44^{-}CD62L^{+}) CD8^{+} T cells and OT-I Tmem subsets. Right shows fold difference in %Ki67^{+} cells between CX3CR1^{int} (int) and CX3CR1^{-} (neg) or CX3CR1^{hi} (hi) Tmem.

(F) Experimental protocol and phenotype of OT-I Tmem cells recovered from spleen and LNs. Mean + SD.

(A–F) n = 2 experiments pooled. *p < 0.05, **p < 0.01, ***p < 0.001 by regular (A) or repeated-measures (E, Blood & Spleen) one-way ANOVA with Tukey's multiple comparisons test or two-tailed t test (E, LN). See also Figures S4C–S4E.

mathematical modeling of the CX3CR1^{int}→CX3CR1^{-} conversion dynamics. Thus, having experimentally validated our mathematical model, we applied the same strategy to simulate the interval between days 128–350 post infection. Our simulations predict that ~56% of CX3CR1^{-} Tcm cells will have arisen from CX3CR1^{int} Tmem cells during this time frame (Figure S4E), indicating that the steady expansion of the CX3CR1^{-} Tmem pool (Figure 3C) is primarily a consequence of CX3CR1^{int}→CX3CR1^{-} Tmem subset conversion.

High Expression Levels of CX3CR1 Positively Identify Tem Cells

Next, we asked how CX3CR1 levels on Tmem cells relate to classical Tcm and Tem subsets that were originally identified in human blood by their differential expression of CCR7 (Sallusto et al., 1999). In our hands, commercially available antibodies to murine CCR7 did not allow a distinction between CCR7^{+} and CCR7^{-} Tmem cells. However, CX3CR1^{-} and CX3CR1^{int} Tmem cells migrated vigorously toward the CCR7 ligand CCL19, whereas the CX3CR1^{hi} subset showed poor chemotaxis (Figure 4A), indicating that CX3CR1^{hi} Tmem cells express little or no functional CCR7. Furthermore, CX3CR1^{hi} Tmem cells were absent from LNs, even though they were abundant in spleen, blood, lung, liver, and bone marrow (Figure 4B). Furthermore, CX3CR1^{hi} Tmem cells expanded less than CX3CR1^{-} and CX3CR1^{int} Tmem cells upon secondary infection (Figure 4C) and, upon in vitro restimulation, were poor producers of IL-2 and killed Ag-pulsed targets more efficiently than other Tmem subsets (Figure S5). As all of these phenotypic and functional features are characteristic of Tem cells (Sallusto et al., 2004; Sallusto et al., 1999), we conclude that high levels of CX3CR1 identify classical Tem cells, and we will henceforth use this term when referring to the CX3CR1^{hi} Tmem subset.

Two LN Homing Tmem Subsets

The CX3CR1^{-} and CX3CR1^{int} Tmem subsets were both responsive to CCL19 and detectable in LNs (Figures 4A and 4B). This implied that T cells that are commonly referred to as Tcm cells consist of two subsets distinguishable by CX3CR1 expression, a heterogeneity that was previously undetectable because both subsets expressed other differentiation-associated markers and transcription factors similarly (Figure S6).

Of note, previous studies have identified other surface markers, such as KLRG1 and the 1B11 glycoform of CD43 to delineate functionally distinct CD8^{+} Tmem subsets (Hikono et al., 2007; Olson et al., 2013). 1B11 expression tended to be lower on CX3CR1^{hi} Tem cells, but did not discriminate CD27^{+}CX3CR1^{-} from CD27^{+}CX3CR1^{int} Tmem cells, which both expressed CD43 variably (Figures S7A–S7D). Nearly all KLRG1^{+} Tmem cells were CX3CR1^{hi}, but the inverse was not the case; depending on the infection model, only ~40%–70% of CX3CR1^{hi} Tem cells expressed KLRG1 (Figure S6A). Thus, a separation of CD8^{+} Tmem cells based on CX3CR1, ideally aided by costaining with CD27 or CXCR3, defines Tmem populations that are not delineated by other known marker combinations.

Differential Regulation of CD62L on Tmem Subsets

CD62L, like CCR7, is required for lymphocyte homing to resting LNs and is often used as surrogate for CCR7 to separate murine Tcm (CD62L^{+}) and Tem (CD62L^{-}) cells. However, a sizeable fraction of CCR7^{+} Tmem cells does not express CD62L, and vice versa (Sallusto et al., 1999). So, a Tcm definition that is based on either homing receptor alone identifies overlapping, but not identical populations, and does not necessarily predict LN homing capacity, which requires co-expression of both molecules (Weninger et al., 2001). Moreover, the use of CD62L to delineate Tcm cells is complicated by the fact that almost all anti-viral Teff cells are initially CD62L^{-}, and the frequency of Ag-experienced CD62L^{+} cells increases gradually during the memory phase (Badovinac et al., 2007; Wherry et al., 2003). The frequency of CD62L^{+} cells and CD62L mean fluorescence intensity were higher among CX3CR1^{-} than CX3CR1^{int} Tmem cells (Figure 4D, S6B and S6C and S7E–S7H), and the kinetics and extent of CD62L re-expression after viral infection differed between the three CX3CR1-defined Tmem subsets (Figure 4E): a substantial fraction of CX3CR1^{-} cells acquired CD62L rapidly (reaching a half maximum after ~20 days) and most cells (~80%) were CD62L^{+} on day 100 post infection; among CX3CR1^{int} Tmem cells, the CD62L^{+} fraction increased more slowly (half maximum after ~55 days) and only ~half ultimately became CD62L^{+}; by contrast, CX3CR1^{hi} Tem cells remained permanently CD62L^{-} (Figures 4D and 4E), consistent with their absence from LNs (Figure 4B).

Whether the progressive increase in CD62L^{+} cells in the early memory phase reflects re-acquisition of CD62L by CD62L^{-} memory precursors or selective outgrowth of a CD62L^{+} Teff subset has long been debated (Marzo et al., 2005; Wherry et al., 2003). To address this, we infected *Cx3cr1*$^{+/gfp}$ mice (CD45.1^{+}) with LCMV and, 30 days later, sorted Ag-experienced (CD44^{hi}) CD8^{+} T cell subsets based on CD62L and CX3CR1 expression (Figure 4F and S7H) and transferred each subset into separate congenic recipients. We performed this experiment with endogenous Tmem cells because supra-physiologic numbers of TCR-tg precursors can skew CD8^{+} T cell differentiation (Marzo et al., 2005; Wherry et al., 2003). When CD62L expression was analyzed on gp33-specific CD45.1^{+} T cells after 30 days, nearly all transferred CD62L^{+}CX3CR1^{-} and CD62L^{-}CX3CR1^{hi} Tmem cells remained CD62L^{+} and CD62L^{-}, respectively, indicating that these subsets are phenotypically stable at steady state. By contrast, a sizeable fraction of transferred CD62L^{-}CX3CR1^{-} and CD62L^{-}CX3CR1^{int} Tmem cells acquired CD62L, although CX3CR1^{-} cells were more efficient at re-expressing CD62L than CX3CR1^{int} cells (Figure 4F). CD62L re-acquisition on transferred CX3CR1^{int} Tmem cells was not restricted to progeny that became CX3CR1^{-}, but was also apparent on cells that remained CX3CR1^{int}.

To assess whether the differential regulation of CD62L on CX3CR1^{-} and CX3CR1^{int} Tmem cells was reflected in their ability to access resting LNs via HEVs, we performed i.v. transfers of mixed Tmem subsets into naive hosts and, after 2 hr, assessed the ratio of CX3CR1^{-} versus CX3CR1^{int} Tmem cells in LNs, spleen, and blood relative to their input ratio. Consistent with the differential CD62L expression, CX3CR1^{-} cells homed to LNs twice more frequently than CX3CR1^{int} Tmem cells, but CX3CR1^{int} cells were twice more frequent in blood, and both subsets were equally represented in the spleen (Figure 4G).

In aggregate, the above results indicate that three discrete Tmem populations exist at steady state in blood and lymphoid

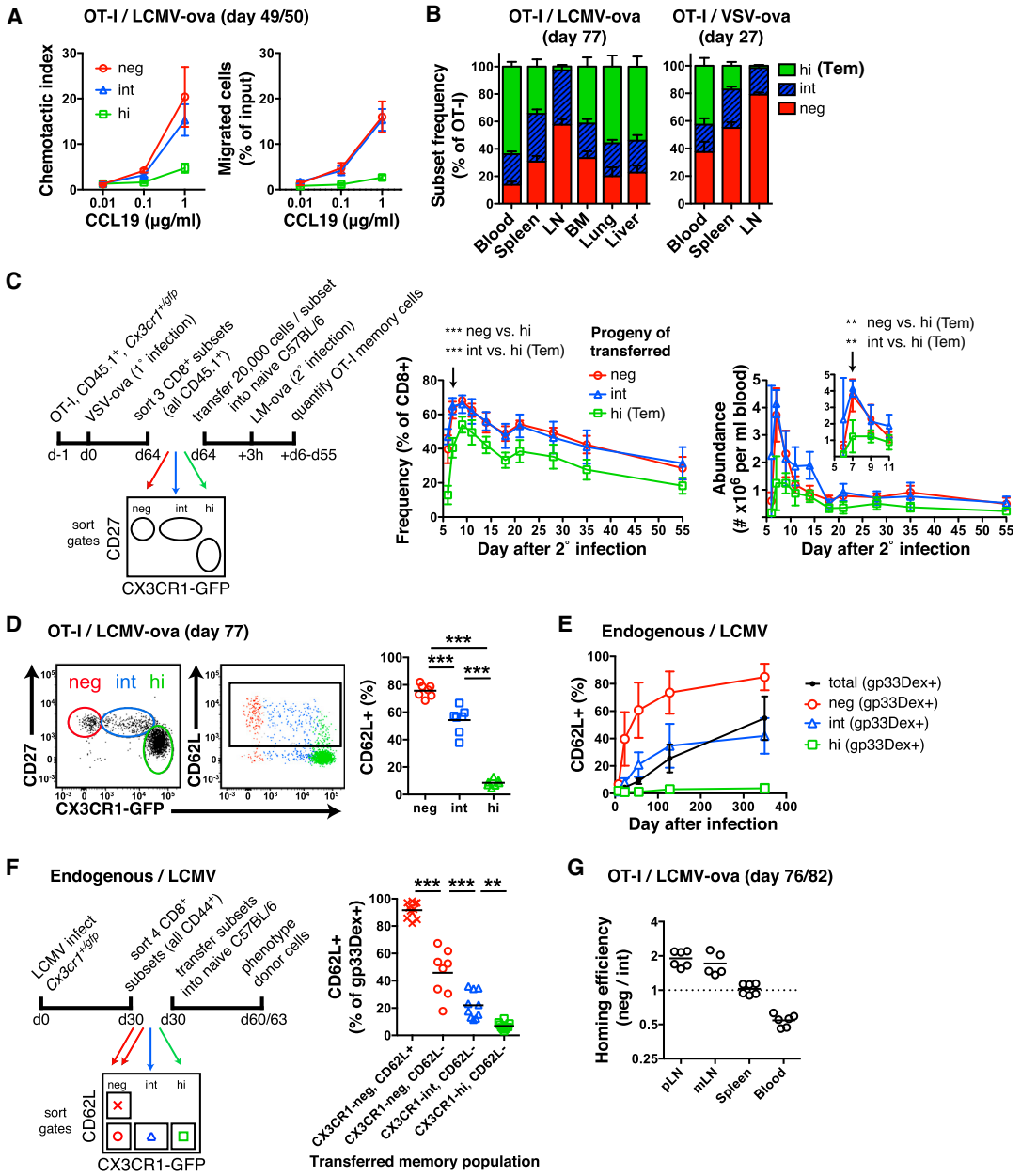

Figure 4. CX3CR1 Levels on Tmem Cells Distinguish Tcm and Tem Cells and a CX3CR1^{int} Tmem Population that, Unlike Tem cells, Re-acquires CD62L

(A) Chemotactic response of OT-I Tmem subsets to CCL19 in a Transwell assay. Chemotactic index shows number of Tmem that migrated toward CCL19 relative to medium alone. 4–5 wells per group per experiment. Mean ± SEM.

(B) OT-I Tmem subset frequencies in lymphoid and non-lymphoid tissues. Mean + SD.

(C) Experimental protocol and frequency of OT-I Tmem cells in blood after secondary infection. Mean ± SD.

(D) Composite FACS plots and CD62L expression on OT-I Tmem in blood.

(E) *Cx3cr1*$^{+/gfp}$ mice were infected with LCMV. CD62L expression on blood circulating gp33-Dextramer^{+} CD8^{+} Tmem cells (total) or subsets thereof. Mean ± SD.

(F) Experimental protocol and frequency of CD62L^{+} cells among recovered splenic and LN resident OT-I Tmem.

(G) Homing efficiency of adoptively transferred Tmem cells to peripheral LN (pLN), mesenteric LN (mLN) and spleen in 2 hr period. # recovered CX3CR1^{-} / # recovered CX3CR1^{int} relative to input ratio.

(A–E, G) n = 2 and (F) n = 3 experiments pooled. **p < 0.01, ***p < 0.001 by one-way ANOVA with Tukey's multiple comparisons test. See also Figures S4C–S7.

tissues: CX3CR1^{hi} cells correspond to classical Tem cells and retain a CD62L^{-}CCR7^{-}CX3CR1^{hi} phenotype for at least 1 year after an acute infection. These bona fide Tem cells do not convert to any of the other subsets (Figure 3D) and are incapable of CD62L re-expression (Figure 4F). Both CX3CR1^{-} and CX3CR1^{int} Tmem cells express CCR7, re-acquire CD62L and

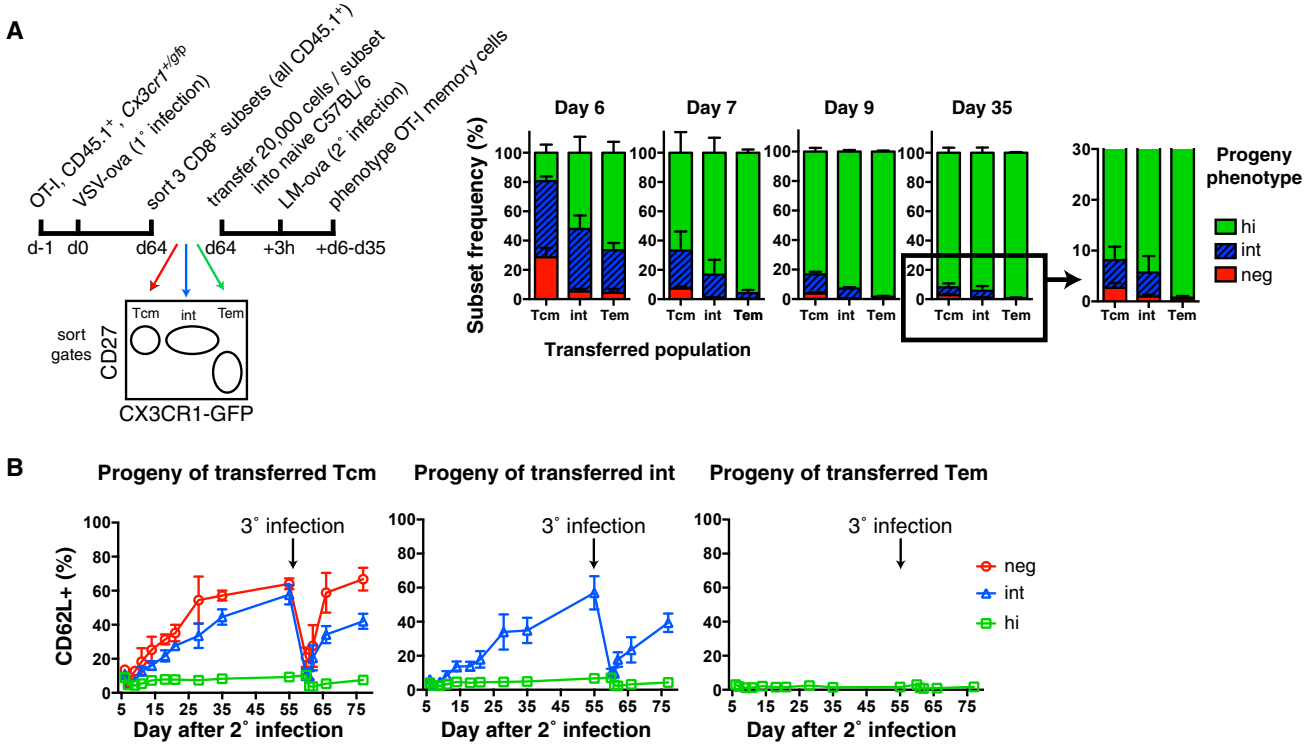

Figure 5. Unidirectional Differentiation from Tcm to CX3CR1^{int} Tmem to Tem after Re-challenge

(A) Experimental protocol and phenotype of OT-I Tmem cells post 2° infection in blood. Mean + SD.

(B) At day 55 post 2° infection, C57BL/6 recipient mice were reinfected with LM-ova (3° infection). Appearance of CD62L^{+} cells on transferred subsets over time. Mean ± SD; n = 2 experiments pooled.

populate resting LNs. However, these subsets are functionally distinct: CX3CR1^{int} Tmem cells have superior steady-state self-renewal capacity (Figure 3E), and CX3CR1^{-} Tmem cells are more prevalent in LNs (Figure 4B), re-acquire CD62L faster and to a greater extent (Figures 4E and 4F), home to resting LNs more efficiently (Figure 4G), contain the highest fraction of IL-2 producers and are the least cytotoxic (Figure S5). These properties of CX3CR1^{-} Tmem cells correspond closely to the properties that traditionally have been ascribed to Tcm cells. Thus, for the purpose of this study, we restrict the Tcm denomination to the CX3CR1^{-} subset and, for now, refer to the CX3CR1^{int} population as such.

Response of Tcm, CX3CR1^{int} Tmem, and Tem Cells to Ag Re-challenge

The results regarding phenotypic stability of resting Tmem subsets differed from those obtained after transfer of Teff subsets, which had implied a uni-directional CX3CR1^{-}→CX3CR1^{int}→CX3CR1^{hi} differentiation at the Teff→Tmem transition (Figures 3A and 3B). In these experiments, transferred Teff cells likely encountered cognate Ag in the host, which promoted their further differentiation. Once Ag was cleared and inflammation waned, however, CX3CR1^{-} Tcm and CX3CR1^{hi} Tem cells were phenotypically stable, and CX3CR1^{int} cells even produced CX3CR1^{-} Tcm cells (Figure 3D).

To address whether each Tmem subset, once formed, is locked in its phenotype, we sorted VSV-ova induced OT-I Tmem subsets and transferred them to naive mice that were then challenged with LM-ova (Figure 5A). Early after secondary infection, all recipients contained GFP^{dim} OT-I cells that had largely disappeared by day 9 and 35 when > 80% and > 90%, respectively, of the recovered cells were CX3CR1^{hi}. The transient dip in GFP expression possibly reflects reduced CX3CR1 biosynthesis or dilution of GFP in rapidly dividing lymphoblasts. Nevertheless, at every time point, the composition of each Tmem subset's progeny was different: CX3CR1^{-} Tcm cells generated small but detectable populations of CX3CR1^{-} and CX3CR1^{int} cells, whereas reactivated CX3CR1^{int} cells only generated CX3CR1^{int} and CX3CR1^{hi} progeny. CX3CR1^{hi} Tem (like Tcm and CX3CR1^{int} Tmem cells) gave rise to numerous CX3CR1^{hi} cells, but generated no other subset. Thus, Ag re-challenge of Tmem cells reinvokes a unidirectional differentiation program, whereby CX3CR1^{-} Tcm cells produce every Tmem population, re-activated CX3CR1^{int} cells generate (at least transiently) only CX3CR1^{int} and CX3CR1^{hi} Tmem cells, and CX3CR1^{hi} Tem cells exclusively give rise to more Tem cells. However, it is likely that once the secondary CX3CR1^{int} Tmem cells have returned to a resting state, they commence to produce CX3CR1^{-} offspring, similar to the primary CX3CR1^{int} Tmem subset (Figure 3D).

Akin to primary infection, secondary infection resulted in a global loss of CD62L, but the CX3CR1^{-} and CX3CR1^{int} progeny of Tcm and CX3CR1^{int} Tmem cells re-acquired CD62L within a few weeks, whereas CX3CR1^{hi} cells remained permanently

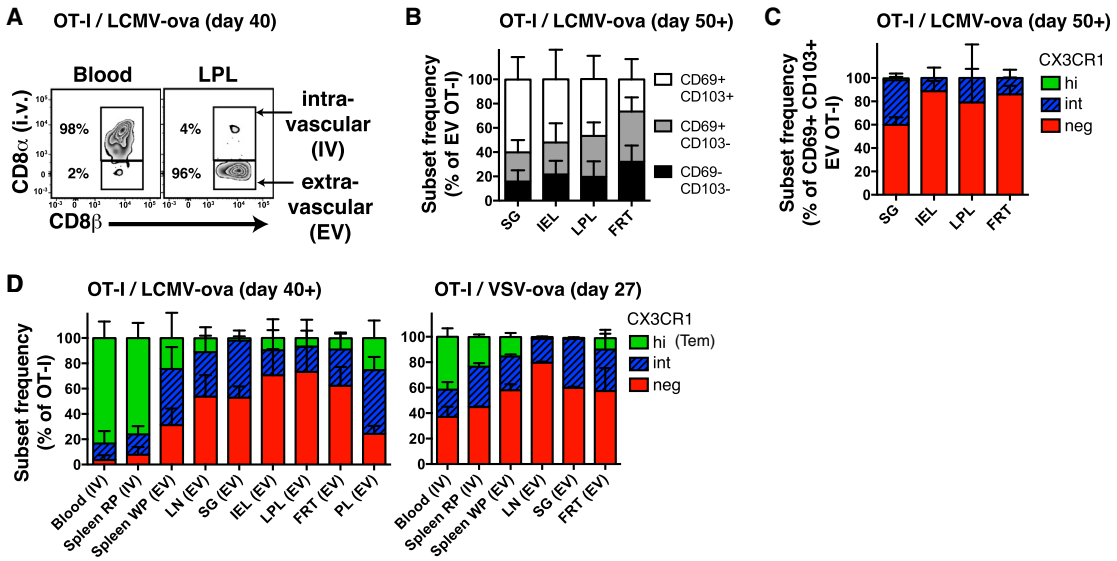

Figure 6. Peripheral Tissues Are Largely Devoid of Tem

Naive OT-I *Cx3cr1*$^{+/gfp}$ CD45.1^{+} T cells were transferred into C57BL/6 followed by LCMV-ova or VSV-ova infection.

(A) Gating strategy for intra- and extra-vascular OT-I cells. Composite FACS plot.

(B) CD69 and CD103 expression on extra-vascular OT-I Tmem cells and (C) frequency of CX3CR1 subsets among extra-vascular CD69^{+}CD103^{+} OT-I Tmem cells in indicated tissues. (B and C) Mean + SD; n = 2 experiments.

(D) Frequency of CX3CR1 subsets among OT-I Tmem cells. Mean + SD. Left: n = 4 experiments (Blood, Spleen, LN, SG) n = 3 experiments (IEL, LPL, FRT). Right: 1 experiment.

CD62L^{-} regardless of the Tmem subset from which they were derived (Figure 5B). This pattern was repeated after tertiary infection of the same mice, suggesting that Tcm and CX3CR1^{int} Tmem cells have the capacity to "remember" their tropism for LNs even after multiple challenges. Thus, CX3CR1 expression levels are inversely correlated with the propensity of CD62L^{-} T cells to re-acquire CD62L after each Ag encounter.

Tem Cells Are Largely Excluded from Peripheral Tissues

Having determined the lineage relationships and LN homing properties of the three blood circulating Tmem subsets, we set out to investigate each population's ability to survey the extravascular space of non-lymphoid tissues and their relationship to Trm cells. Extravascular Tmem cells comprise a mixture of two populations: (1) tissue-confined Trm cells that express CD69 and/or CD103, receptors that retain them within tissues (Fletcher et al., 2011; Mueller et al., 2013; Steinert et al., 2015), and (2) phenotypically poorly defined migratory Tmem cells that visit non-lymphoid tissues transiently and return to the blood via draining lymphatics and TD.

We analyzed the phenotype of OT-I Tmem cells within the extravascular compartment of non-lymphoid tissues, including the salivary gland (SG), the female reproductive tract (FRT), and the intra-epithelial lymphocytes (IEL) and lamina propria lymphocytes (LPL) in the small intestine. Intra- and extravascular Tmem cells were distinguished by flow cytometry after i.v. injection of anti-CD8α mAb shortly before sacrificing the mouse (Figure 6A). With this strategy, extravascular cells are inaccessible to the mAb and remain unstained (Anderson et al., 2014).

There was considerable heterogeneity among extravascular OT-I Tmem cells, with 70%–80% expressing CD69 and roughly half co-expressing CD103, while 20%–30% expressed neither marker (Figure 6B). Most extravascular CD69^{+}CD103^{+} OT-I Trm cells were CX3CR1^{-} (60%–90%) and the remainder was CX3CR1^{int} (Figure 6C). This phenotype is consistent with previous findings that peripheral tissues in LCMV infected mice are seeded before day 7 post infection (Masopust et al., 2010), a period during which most Teff cells are still CX3CR1^{-} or CX3CR1^{int} (Figure 1D). Thus, Trm precursors apparently do not upregulate CX3CR1 once they have accessed a peripheral tissue, even during an ongoing infection. Furthermore, the fact that Trm cells were entirely devoid of CX3CR1^{hi} cells suggested that this population is neither derived from nor replenished by Tem cells. Even among all extravascular Tmem cells (i.e., without gating on CD69 or CD103), CX3CR1^{hi} T cells were almost completely absent, except in peritoneal lavage fluid (Figure 6D).

CX3CR1^{int} Tmem Cells Are the Predominant Subset Circulating through Peripheral Tissues

That Tmem cells egress from peripheral tissues via the draining lymphatics has been documented in sheep (Mackay et al., 1990) and humans (Hunger et al., 1999), but the precise phenotype of these migratory cells has been unclear. The finding that CX3CR1^{hi} Tmem cells are largely excluded from peripheral tissues seemed at odds with the idea that Tem cells are the principal subset surveying those tissues. Two scenarios seemed plausible to explain our findings: first, if Tem cells were uniquely capable of accessing peripheral tissues, they would have to do so only rarely and/or spend very little time before departing via the draining lymphatics. Second, contrary to current belief, a Tmem subset other than CX3CR1^{hi} Tem cells might be responsible for peripheral immune surveillance. To test these two

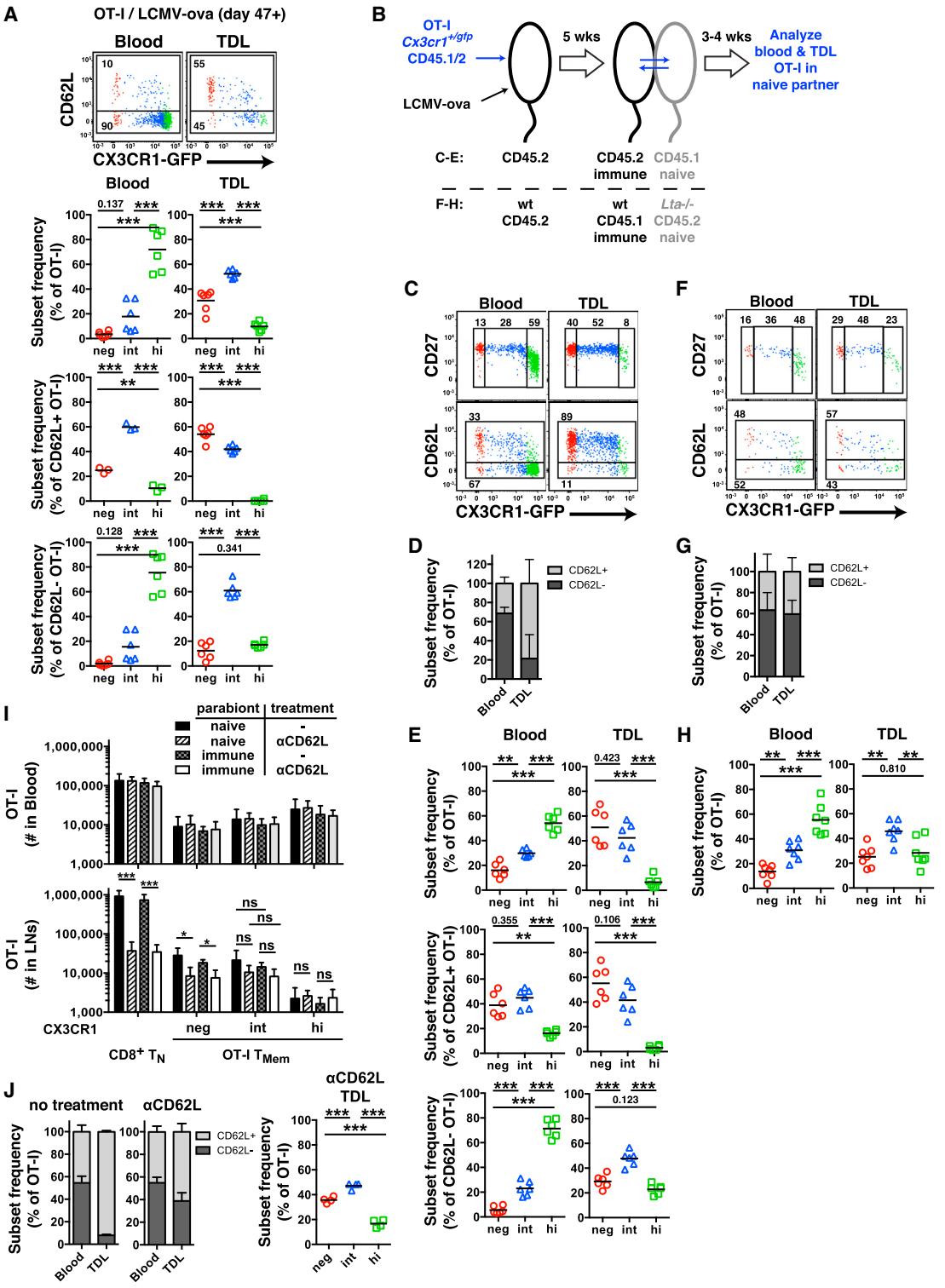

Figure 7. CX3CR1^{int} Tmem Cells, Not Tem cells, Are the Major Tmem Subset Circulating through Peripheral Tissues

For a Figure360 author presentation of Figure 7, see http://dx.doi.org/10.1016/j.immuni.2016.10.018#mmc3.

(A) OT-I Tmem subsets in blood (left) and TDL (right). FACS plots above were concatenated from three immunized mice. Data panels below show frequency of CX3CR1^{-} (red), CX3CR1^{int} (blue), and CX3CR1^{hi} (green) Tmem subsets among total (top), CD62L^{+} (middle), and CD62L^{-} (bottom) OT-I Tmem cells.

(B) Schematic for parabiosis experiments in (C)–(H).

(C and F) FACS plots depicting blood- and lymph-borne OT-I Tmem cells in naive WT (C) and *Lta*$^{-/-}$ (F) parabionts. Numbers show percentage of gated events.

(D and G) Frequency of CD62L^{+} and CD62L^{-} OT-I Tmem cells (mean + SD).

(legend continued on next page)

alternatives, we collected TD lymph (TDL) from immunized mice to characterize the migratory Tmem cells en route toward the blood.

The TD collects lymph from all tissues below the diaphragm and the left upper body. It is a conduit for migratory Tmem cells that leave peripheral tissues via the afferent lymph, pass through regional LNs and ultimately return to the blood. In addition, TDL contains lymphocytes that recirculate via HEVs through secondary lymphoid organs (SLOs) (Gowans and Knight, 1964). Homing via resting HEVs requires lymphocyte-expressed CD62L, while trafficking to most non-lymphoid tissues is CD62L independent (von Andrian and Mackay, 2000). Thus, most CD62L$^-$ Tmem cells in TDL are unlikely to have accessed the lymph after homing via HEVs and, therefore, should represent the migratory peripheral Tmem subset.

Indeed, at 7 weeks after LCMV-ova infection, 56.2% ± 17.4% (mean ± SD) of OT-I Tmem cells in TDL were CD62L$^-$, suggesting that the number of Tcm cells that migrate through LNs is approximately equal to that of the peripheral migratory Tmem subset (Figure 7A). Consistent with our earlier data (Figure 3C and 4B), peripheral blood Tmem cells were dominated by CD62L$^-$CX3CR1^{hi} Tem cells. In contrast, the most abundant subset in TDL were CX3CR1^{int} Tmem cells. The CD62L$^+$ (i.e., LN homing) OT-I fraction in TDL contained slightly more CX3CR1$^-$ Tcm than CX3CR1^{int} Tmem cells and was devoid of CX3CR1^{hi} Tem cells (Figure 7A), consistent with the differential appearance of these subsets in LNs (Figure 4B). The CD62L$^-$ (periphery derived) Tmem fraction was dominated by CX3CR1^{int} Tmem cells, which were 3–4 times more frequent than CX3CR1$^-$ Tcm or CX3CR1^{hi} Tem cells.

While these results implied that not Tem, but CX3CR1^{int} Tmem cells are the predominant subset trafficking through peripheral tissues, it was important to verify that the CD62L$^-$ Tmem cells in TDL were truly recirculating. Conceivably, some could have been progeny of in situ dividing Trm cells. To address this, we generated parabiotic pairs of congenic mice, which establish a shared circulation, allowing exchange of hematopoietic cells between conjoined partners (Wright et al., 2001). WT mice (CD45.2) received OT-Ix*Cx3cr1*$^{+/gfp}$ Tn cells (CD45.1/2) and were then infected with LCMV-ova to generate Tmem cells (Figure 7B). After 5 weeks, each immunized animal was surgically joined to a naive partner (CD45.1), which underwent TD cannulation 3–4 weeks later. Because the naive parabiont by definition does not harbor Trm cells, any OT-I cell in its TDL should remain free of Trm progeny and thus reflect exclusively migratory Tmem cells.

Consistent with our findings in non-parabiotic mice, CX3CR1^{int} Tmem cells were the most abundant subset among periphery-derived CD62L$^-$ Tmem cells in TDL of naive parabionts. This is in stark contrast with the blood, which was dominated by CD62L$^-$CX3CR1^{hi} Tem cells (Figures 7C–7E). Thus, blood-derived Tmem cells, primarily the CX3CR1^{int} subset, traverse host tissues in a CD62L-independent fashion and return to the blood via the lymph.

Although CD62L is required for most T cells to interact with HEVs, some mucosal lymphoid tissues, such as Peyer's patches, can support CD62L-independent lymphocyte homing (Bargatze et al., 1995). To rule out that CD62L$^-$ Tmem cells had entered the TDL pool after using alternate adhesion pathways to home to SLOs rather than migrating across peripheral tissues, we generated parabiotic pairs of immune wild-type mice containing OT-Ix*Cx3cr1*$^{+/gfp}$ Tmem cells and naive lymphotoxin-α deficient (*Lta*$^{-/-}$) mice, which lack all SLOs except the spleen (Figure 7B). Any Tmem cell in TDL of the *Lta*$^{-/-}$ partner must have accessed the lymph after trafficking from the blood through a non-lymphoid tissue, regardless of CD62L expression. The TDL of naive *Lta*$^{-/-}$ parabionts contained ~40% CD62L$^+$ OT-I Tmem cells (Figures 7F and 7G), indicating that also CD62L$^+$ Tmem cells have the capacity to recirculate through non-lymphoid tissues. Notwithstanding, CX3CR1^{int} Tmem cells dominated the total Tmem pool in TDL of *Lta*$^{-/-}$ parabionts (Figure 7H).

These experiments contradict the long-held paradigm that classical Tem cells are specialized to survey non-lymphoid tissues at steady-state. Rather, our results show that the CX3CR1^{int} Tmem subset is the predominant population that recirculates between blood and peripheral tissues.

CX3CR1^{int} Tmem Cells Preferentially Recirculate through LNs via a CD62L Independent Route

A recent study reported that the number of LN-resident CX3CR1$^+$ CD8$^+$ Tmem cells did not change after inhibition of LN homing by anti-CD62L (Böttcher et al., 2015). Thus, it was proposed that CX3CR1$^+$ cells in LNs represent a non-migratory Trm population. Our results suggest a plausible alternative scenario: first, our data indicate that there are two distinct CX3CR1$^+$ Tmem subsets, and only CX3CR1^{int} Tmem cells are detectable in LNs. Second, the fact that CX3CR1^{int} cells traverse peripheral tissues implies that they can access LNs also via afferent lymphatics, a migratory route that might not require CD62L.

To test whether LN-resident CX3CR1^{int} Tmem cells are sessile or migratory, we generated parabiotic pairs of congenic mice by joining immunized animals (containing CD45.2$^+$ OT-Ix*Cx3cr1*$^{+/gfp}$ Tmem) to naive partners (CD45.1$^+$). Two weeks after surgery, half of the pairs were treated with anti-CD62L for 5–7 days. As expected, CD62L blockade reduced the number of polyclonal Tn and CX3CR1$^-$ OT-I Tcm cells in LNs of all parabionts, while leaving T cell subsets in the blood unchanged (Figure 7I). Consistent with previous findings (Böttcher et al., 2015), CD62L inhibition did not significantly alter the frequency of CX3CR1^{int} Tmem cells in LNs of immunized hosts. However, LN CX3CR1^{int} cells were not confined to the immunized parabionts, as would be expected if these Tmem cells were non-migratory. Rather, the LNs of both partners contained equivalent numbers of CX3CR1^{int} cells, irrespective of whether the animals had received anti-CD62L. Thus, CX3CR1^{int} Tmem cells are not sessile in LNs, but actively

(E) Frequency of Tmem subsets among total (top), CD62L$^+$ (middle) and CD62L$^-$ (bottom) OT-I Tmem cells in WT parabionts.
(H) Frequency of Tmem subsets among total OT-I Tmem cells in *Lta*$^{-/-}$ parabionts.
(I) Cell numbers and (J) phenotype of OT-I Tmem cells in pooled axillary, brachial and inguinal LNs from control and anti-CD62L-treated naive and immune parabiotic pairs (mean + SD).
(A, I, J) n = 2 (C–E) n = 4 and (F–H) n = 3 experiments pooled. *p < 0.05, ***p < 0.001 (one-way ANOVA with Tukey's multiple comparisons test).
Figure360: an author presentation of Figure 7.

recirculate through these organs in a CD62L independent fashion, indicating that they enter LNs primarily via afferent lymphatics rather than HEVs.

Of note, ~40% of OT-I Tmem cells recirculating through peripheral tissues of *Lta*$^{-/-}$ parabionts were CD62L^{+} (Figure 7G). Thus, although LN entry through afferent lymphatics is CD62L independent, the presence of CD62L does not preclude co-expression of other traffic molecules that enable Tmem cell recirculation through peripheral tissues, at least in *Lta*$^{-/-}$ hosts. To determine whether CD62L^{+} Tmem cells also recirculate through peripheral tissues in WT mice, we collected TDL of naive C57BL/6 parabionts in which LN entry through HEV was blocked by anti-CD62L. Consequently, TDL of these mice predominantly contained T cells that had circulated through peripheral tissues. Consistent with our data from the *Lta*$^{-/-}$ mice, a substantial fraction (~60%) of OT-I cells in TDL of anti-CD62L treated WT parabionts were CD62L^{+} (Figure 7J), indicating that both CD62L^{-} and CD62L^{+} Tmem cells recirculate through peripheral tissues. Also in this experimental setting, CX3CR1^{int} Tmem cells were the most prominent OT-I Tmem subset in TDL.

DISCUSSION

Until recently, *Cx3cr1*$^{+/gfp}$ mice have been primarily used to distinguish myeloid phagocyte subsets (Geissmann et al., 2003; Jung et al., 2000; Palframan et al., 2001). We observed that many CD8 T cells upregulated CX3CR1 upon pathogen challenge, consistent with a recent study that uncovered profound differences between CX3CR1^{-} and CX3CR1^{+} Tmem cells at the transcriptome, proteome, and functional level (Böttcher et al., 2015). We noted that CX3CR1^{+} CD8^{+} T cells are further divisible into CX3CR1^{int} and CX3CR1^{hi} subsets. Subsetting of CD8^{+} Teff and Tmem cells into CX3CR1^{-}, CX3CR1^{int}, and CX3CR1^{hi} populations allowed us to address several long-standing issues in T cell biology: (1) Our results demonstrate that the Teff differentiation state, as defined by CX3CR1, predicts the Tmem subset(s) that a given Teff cell produces. (2) Our findings shed light on a historic debate on re-expression of CD62L and the origin of Tcm cells. (3) We identify high expression of CX3CR1 as a Tem marker to probe the relationship between Tem and other Tmem subsets. (4) Contrary to the current paradigm, we shows that Tem cells do not survey non-lymphoid tissues at steady-state. (5) Instead, CX3CR1^{int} Tmem are the predominant migratory Tmem subset that patrols through peripheral tissues, accesses afferent lymphatics, traverses the draining LNs, and returns via the TD to the blood.

This study was motivated by the observation that infections induced non-uniform CX3CR1 upregulation on Teff cells. Prior to the induction of CX3CR1^{+} cells, a transient wave of early Teff cells is thought to seed peripheral tissues to give rise to Trm cells (Masopust et al., 2010). We found that Trm cells are CX3CR1$^{-/low}$, suggesting that non-lymphoid tissues are not conducive to the activation of the *Cx3cr1* locus. Of note, in vitro activation of CD8^{+} Tn cells induced only sparse CX3CR1 expression (unpublished observation). The signals that precipitate CX3CR1 upregulation in vivo remain undefined, but are probably restricted to SLOs or the circulatory system where Teff cells are abundant when they acquire CX3CR1.

Our findings address a long-standing conundrum that partially resulted from the use of CD62L to distinguish Tcm and Tem subsets: in one study, TCR-tg CD62L^{-} Tmem cells (considered Tem) were transferred 30 days after infection to naive recipients (Wherry et al., 2003). Some transferred cells acquired CD62L (considered Tcm), so it was proposed that Tcm cells arise along a linear Tn → Teff → Tem → Tcm pathway. Others disputed these conclusions, because endogenous CD62L^{-}CD8^{+} Tmem cells transferred 111 days after viral infection failed to produce CD62L^{+} cells, suggesting that Tcm cells do not arise from Tem cells (Marzo et al., 2005). Indeed, in vitro, weakly activated T cells assume a Tcm phenotype without passing through a bona fide Teff stage (Manjunath et al., 2001). Thus, the origin of Tcm cells has been an unresolved matter of debate.

Our results show that some CD62L^{+} Tcm cells already exist during the initial memory phase, but early CD62L^{-} Tmem cells could re-express CD62L and join the Tcm pool. However, only CX3CR1^{-} (pre-Tcm) and CX3CR1^{int} Tmem cells underwent this CD62L^{-} → CD62L^{+} conversion; CX3CR1^{hi} Tmem cells, the bona fide Tem, were incapable of Tcm differentiation. Moreover, CD62L^{+} Tmem cells plateaued after ~100 days, suggesting that steady-state Tmem cells eventually become locked in a CD62L^{+} or CD62L^{-} state.

Although our characterization of LN homing Tmem subsets relied, in part, on CD62L expression, we note that CD62L mediates only the initial rolling step in the multi-step adhesion cascade. Rolling cells must also engage CCR7 and the integrin LFA-1 to home into LNs via HEVs (von Andrian and Mempel, 2003). Indeed, both CX3CR1^{-} Tcm and CX3CR1^{int} Tmem cells, but not CX3CR1^{hi} Tem cells, responded to the CCR7 ligand CCL19, and both subsets were present in LNs. Anti-CD62L blocked Tn and Tcm cell homing, but did not reduce CX3CR1^{int} Tmem cells in LNs, consistent with a recent study (Böttcher et al., 2015). One plausible explanation for this finding is that intranodal CX3CR1^{+} Tmem cells represent a non-migratory Trm subset. However, our parabiosis experiments show that both Tcm and CX3CR1^{int} Tmem cells traffic continuously to LNs. Thus, CX3CR1^{int} Tmem cells recirculate through LNs independently of CD62L, presumably by entering peripheral tissues that recruit leukocytes through other adhesion pathways (von Andrian and Mackay, 2000). The peripheral Tmem cells might then depart via local lymphatics to access draining LNs through the "backdoor." Although this migratory route does not require CD62L, CX3CR1^{int} Tmem cells presumably depend on CCR7 to enter lymphatics (Bromley et al., 2005; Debes et al., 2005), and to navigate from lymph sinuses within LNs toward the T cell area (von Andrian and Mempel, 2003).

Consistent with the idea that CX3CR1^{int} Tmem cells engage in peripheral immune surveillance, this was the predominant Tmem subset among CD62L^{-} T cells in TDL in both immunized and naive parabionts. It should be cautioned that T cell homing to mucosal SLOs, such as Peyer's patches, does not absolutely require CD62L (von Andrian and Mackay, 2000), so some CD62L^{-} Tmem cells could have reached the TDL of WT mice via SLOs. However, CX3CR1^{int} Tmem cells predominated also in TDL of naive *Lta*$^{-/-}$ parabionts, which lacked all SLOs except the spleen, so partner-derived Tmem cells could only access lymph conduits by migrating through peripheral tissues. This finding unequivocally establishes the CX3CR1^{int} subset as the

major Tmem population engaged in steady-state surveillance of non-lymphoid tissues. By contrast, CX3CR1^{hi} Tem cells, which had long been assumed to perform this function, are under-represented in the Tmem pool in TDL and are confined to the spleen and intravascular compartment.

Our data allow a rough estimate of peripheral tissue surveillance by migratory Tmem cells. The frequency of CD62L^{-}CD8^{+} Tmem cells in TDL (~2.1% of mononuclear leukocytes [MNL]) allows an approximation of the flux of Tmem cells returning from peripheral tissues. Murine TDL collected from the cisterna chyli (reflecting ~half of total efferent lymph flow) contains 2.2 × 10^{6} MNL/ml at a flow rate of 1.2 ml/hr (Ionac et al., 1997). Thus, ~2.7 × 10^{6} CD62L^{-}CD8^{+} Tmem cells return to the blood via the TDL after passing through peripheral tissues per day. The CX3CR1^{int} subset accounts for almost two thirds (61%) or 1.65 × 10^{6} cells per day of this population.

In light of these results, we propose to designate the CX3CR1^{int} Tmem subset "peripheral memory" (tpm) cells. tpm cells exhibit phenotypic, functional, and homeostatic features distinct from classical Tcm and Tem subsets: they are long-lived CX3CR1^{int} Tmem cells that express CD27, CXCR3, and CCR7, as well as variable levels of CD62L. Like Tcm cells, CCR7^{+}CD62L^{+} tpm cells can home to LNs via HEVs, but they appear to access LNs primarily via afferent lymphatics. Indeed, tpm cells are the predominant migratory Tmem subset surveying the periphery. In addition, tpm cells have a higher homeostatic proliferation rate than any other Tmem subset, which allows tpm cells not only to self-renew, but also to produce CX3CR1^{-} Tcm cells that contribute to the steady growth of the Tcm pool. The mechanisms that confer these unique abilities to tpm cells require further investigation. However, Tmem cell self-renewal depends on access to survival signals, such as IL-15 (Becker et al., 2002). It is tempting to speculate that, even though Tcm and tpm cells express similar levels of cytokine receptors, including CD122 (data not shown) and CD127, the broad migratory horizon of tpm cells might provide them with access to proliferation-promoting cytokines that are beyond reach of Tmem cells with more restricted traffic patterns.

Regardless, our findings imply that current concepts of Tmem subset distribution and trafficking require revision. Tcm cells, as described earlier, circulate primarily between blood and SLOs (von Andrian and Mempel, 2003), while tpm cells survey the periphery. By contrast, Tem cells, which had been thought to circulate between blood and peripheral tissues, are actually excluded from most extravascular compartments, except the spleen and, to a moderate degree, the peritoneal cavity. Further work will be needed to clarify the functional consequences of this apparent restriction of Tem cells to the intravascular space.

EXPERIMENTAL PROCEDURES

Mice

C57BL/6, *Cx3cr1*$^{gfp/gfp}$CD45.1$^{+/+}$, CD45.1$^{+/+}$, OT-I, *Tbx21*$^{-/-}$, *Rag1*$^{-/-}$, and *Lta*$^{-/-}$ mice were purchased from Jackson Laboratory and P14 from Taconic farms. *Lta*$^{-/-}$ mice were also kindly provided by Dr. N.H. Ruddle (Yale School of Public Health). All animal experiments were performed in accordance with national and institutional guidelines, and were approved by IACUC and COMS of Harvard Medical School.

T Cell Isolation and Flow Cytometry

T cells were purified by physical dissociation (spleen, lymph nodes, liver, bone marrow) or digestion with 62.5 μg/ml LiberaseTM + 100 μg/ml DNaseI (lung, female reproductive tract, salivary gland) for 20–30 min at 37°C. Livers, lungs, and salivary glands underwent a density gradient (NycoPrepTM 1.077, Axis-Shield).

Intravascular T cells were labeled by i.v. injection of 1–3 μg anti-CD8 mAb 3 min prior to sacrifice. Human lymphocytes were enriched from PBMC of anonymous donors (Research Blood Components, LLC) by density gradient (NycoPrepTM 1.077, Axis-Shield). Staining with fractalkine-Ig, a fusion protein of fractalkine with a human IgG1 Fc fragment (Millennium) was performed for 1 hr at 4°C, followed by anti-human IgG. Gp33-specific CD8 were detected by H-2 Db / KAVYNFATC MHC Dextramers (Immudex).

Cytokine staining employed the Cytofix/CytopermTM Fixation/Permeabilization kit (BD Biosciences), and nuclear staining the Foxp3 Staining Buffer Set (eBioscience). Nuclear stain was performed on either sorted subsets or in combination with CX3CR1 antibody (BioLegend). Cells were stained with anti-rat IgG2a Fab to detect CD62L after treatment of mice with anti-CD62L (MEL-14; rat IgG2a).

Data analysis was performed in FlowJo v10 (Tree Star) and GraphPad Prism 5/6 as described in Supplemental Experimental Procedures.

Surgeries

Parabiosis and TDL collection were performed as previously described (Massberg et al., 2007; Wright et al., 2001). To block CD62L-dependent LN entry, both parabiotic partners received 100 μg MEL-14 i.p. every 2–3 days.

Infections

Mice were infected i.v. with 10^{3}–10^{4} focus forming units (ffu) LCMV Armstrong (abbreviated LCMV), 0.5–1 × 10^{4} ffu LCMV Armstrong expressing katushka and ovalbumin (LCMV-ova), 2 × 10^{6} plaque forming units (pfu) VSV expressing ovalbumin (VSV-ova), or 10^{3} (1° infection) – 10^{5} (2° & 3° infection) colony-forming units (cfu) *Listeria monocytogenes* expressing ovalbumin (Dudani et al., 2002)(LM-ova). All infectious work was performed in accordance with national and institutional guidelines.

Chemotaxis, Killing, and Homing Assay

Migration toward CCL19 (R&D Systems) was assessed using Transwell plates, (Corning Incorporated). Antigen-specific target lysis was determined in vitro. The LN homing efficiency was determined 2 hr after i.v. adoptive transfer.

Supplemental Information

The supplement provides details on the gender and age of mice, transferred cell numbers, IEL and LPL isolation, surgery, antibody clones, sort purity, LCMV-ova generation, in vitro assays, statistics, and mathematical modeling.

SUPPLEMENTAL INFORMATION

Supplemental Information includes seven figures and Supplemental Experimental Procedures and can be found with this article online at http://dx.doi.org/10.1016/j.immuni.2016.10.018.

AUTHOR CONTRIBUTIONS

C.G. designed and performed experiments, analyzed data, and wrote the paper. E.A.M. initiated the study, designed and performed experiments, and analyzed data. S.M.L. and D.A. designed and performed experiments and analyzed data. A.J.Z. and L.W. performed experiments. R.G. performed mathematical modeling. J.C.dlT. created LCMV-ova. U.H.v.A. supervised the study, designed experiments, and wrote the paper.

ACKNOWLEDGMENTS

The authors thank N.H. Ruddle for *Lta*$^{-/-}$ mice, D. Higgins for LM-ova, I.B. Mazo, R.J. Gonzales, and M. Perro for technical assistance, and A.K. Chakraborty, A. Thiriot, and Y. Nemoto for fruitful discussions. This study was supported by a Rubicon fellowship (Netherlands Organization for Scientific Research, NWO) and a postdoctoral fellowship of the Cancer Research

Institute Irvington Fellowship Program to C.G., NIH T32 Training Grant in Hematology HL07623-20 to E.A.M., NIH F31 grant CA171339 to S.M.L., NIH T32 grant HL066987 to D.A., the Ragon Institute of MGH, MIT, and Harvard, the HMS Center for Immune Imaging, and NIH/NIAID RO1 AI069259, PO1 AI078897 and PO1 AI112521 to U.H.v.A.

Received: April 13, 2016
Revised: August 6, 2016
Accepted: August 26, 2016
Published: December 6, 2016

REFERENCES

Anderson, K.G., Mayer-Barber, K., Sung, H., Beura, L., James, B.R., Taylor, J.J., Qunaj, L., Griffith, T.S., Vezys, V., Barber, D.L., and Masopust, D. (2014). Intravascular staining for discrimination of vascular and tissue leukocytes. Nat. Protoc. *9*, 209–222.

Badovinac, V.P., Haring, J.S., and Harty, J.T. (2007). Initial T cell receptor transgenic cell precursor frequency dictates critical aspects of the CD8(+) T cell response to infection. Immunity *26*, 827–841.

Bargatze, R.F., Jutila, M.A., and Butcher, E.C. (1995). Distinct roles of L-selectin and integrins α 4 β 7 and LFA-1 in lymphocyte homing to Peyer's patch-HEV in situ: the multistep model confirmed and refined. Immunity *3*, 99–108.

Becker, T.C., Wherry, E.J., Boone, D., Murali-Krishna, K., Antia, R., Ma, A., and Ahmed, R. (2002). Interleukin 15 is required for proliferative renewal of virus-specific memory CD8 T cells. J. Exp. Med. *195*, 1541–1548.

Böttcher, J.P., Beyer, M., Meissner, F., Abdullah, Z., Sander, J., Höchst, B., Eickhoff, S., Rieckmann, J.C., Russo, C., Bauer, T., et al. (2015). Functional classification of memory CD8(+) T cells by CX3CR1 expression. Nat. Commun. *6*, 8306.

Bromley, S.K., Thomas, S.Y., and Luster, A.D. (2005). Chemokine receptor CCR7 guides T cell exit from peripheral tissues and entry into afferent lymphatics. Nat. Immunol. *6*, 895–901.

Debes, G.F., Arnold, C.N., Young, A.J., Krautwald, S., Lipp, M., Hay, J.B., and Butcher, E.C. (2005). Chemokine receptor CCR7 required for T lymphocyte exit from peripheral tissues. Nat. Immunol. *6*, 889–894.

Dudani, R., Chapdelaine, Y., Faassen Hv, Hv., Smith, D.K., Shen, H., Krishnan, L., and Sad, S. (2002). Multiple mechanisms compensate to enhance tumor-protective CD8(+) T cell response in the long-term despite poor CD8(+) T cell priming initially: comparison between an acute versus a chronic intracellular bacterium expressing a model antigen. J. Immunol. *168*, 5737–5745.

Fletcher, A.L., Malhotra, D., Acton, S.E., Lukacs-Kornek, V., Bellemare-Pelletier, A., Curry, M., Armant, M., and Turley, S.J. (2011). Reproducible isolation of lymph node stromal cells reveals site-dependent differences in fibroblastic reticular cells. Front. Immunol. *2*, 35.

Geissmann, F., Jung, S., and Littman, D.R. (2003). Blood monocytes consist of two principal subsets with distinct migratory properties. Immunity *19*, 71–82.

Gerdes, J., Lemke, H., Baisch, H., Wacker, H.H., Schwab, U., and Stein, H. (1984). Cell cycle analysis of a cell proliferation-associated human nuclear antigen defined by the monoclonal antibody Ki-67. J. Immunol. *133*, 1710–1715.

Gerlach, C., van Heijst, J.W., and Schumacher, T.N. (2011). The descent of memory T cells. Ann. N Y Acad. Sci. *1217*, 139–153.

Gowans, J.L., and Knight, E.J. (1964). The route of re-circulation of lymphocytes in the rat. Proc. R. Soc. Lond. B Biol. Sci. *159*, 257–282.

Hamann, D., Baars, P.A., Rep, M.H., Hooibrink, B., Kerkhof-Garde, S.R., Klein, M.R., and van Lier, R.A. (1997). Phenotypic and functional separation of memory and effector human CD8+ T cells. J. Exp. Med. *186*, 1407–1418.

Hikono, H., Kohlmeier, J.E., Takamura, S., Wittmer, S.T., Roberts, A.D., and Woodland, D.L. (2007). Activation phenotype, rather than central- or effector-memory phenotype, predicts the recall efficacy of memory CD8+ T cells. J. Exp. Med. *204*, 1625–1636.

Hintzen, R.Q., de Jong, R., Lens, S.M., Brouwer, M., Baars, P., and van Lier, R.A. (1993). Regulation of CD27 expression on subsets of mature T-lymphocytes. J. Immunol. *151*, 2426–2435.

Hunger, R.E., Yawalkar, N., Braathen, L.R., and Brand, C.U. (1999). The HECA-452 epitope is highly expressed on lymph cells derived from human skin. Br. J. Dermatol. *141*, 565–569.

Ionac, M., Laskay, T., Labahn, D., Geisslinger, G., and Solbach, W. (1997). Improved technique for cannulation of the murine thoracic duct: a valuable tool for the dissection of immune responses. J. Immunol. Methods *202*, 35–40.

Jameson, S.C., and Masopust, D. (2009). Diversity in T cell memory: an embarrassment of riches. Immunity *31*, 859–871.

Jiang, X., Clark, R.A., Liu, L., Wagers, A.J., Fuhlbrigge, R.C., and Kupper, T.S. (2012). Skin infection generates non-migratory memory CD8+ T(RM) cells providing global skin immunity. Nature *483*, 227–231.

Joshi, N.S., Cui, W., Chandele, A., Lee, H.K., Urso, D.R., Hagman, J., Gapin, L., and Kaech, S.M. (2007). Inflammation directs memory precursor and short-lived effector CD8(+) T cell fates via the graded expression of T-bet transcription factor. Immunity *27*, 281–295.

Jung, S., Aliberti, J., Graemmel, P., Sunshine, M.J., Kreutzberg, G.W., Sher, A., and Littman, D.R. (2000). Analysis of fractalkine receptor CX(3)CR1 function by targeted deletion and green fluorescent protein reporter gene insertion. Mol. Cell. Biol. *20*, 4106–4114.

Kaech, S.M., Tan, J.T., Wherry, E.J., Konieczny, B.T., Surh, C.D., and Ahmed, R. (2003). Selective expression of the interleukin 7 receptor identifies effector CD8 T cells that give rise to long-lived memory cells. Nat. Immunol. *4*, 1191–1198.

Mackay, C.R., Marston, W.L., and Dudler, L. (1990). Naive and memory T cells show distinct pathways of lymphocyte recirculation. J. Exp. Med. *171*, 801–817.

Mackay, L.K., Rahimpour, A., Ma, J.Z., Collins, N., Stock, A.T., Hafon, M.L., Vega-Ramos, J., Lauzurica, P., Mueller, S.N., Stefanovic, T., et al. (2013). The developmental pathway for CD103(+)CD8+ tissue-resident memory T cells of skin. Nat. Immunol. *14*, 1294–1301.

Manjunath, N., Shankar, P., Wan, J., Weninger, W., Crowley, M.A., Hieshima, K., Springer, T.A., Fan, X., Shen, H., Lieberman, J., and von Andrian, U.H. (2001). Effector differentiation is not prerequisite for generation of memory cytotoxic T lymphocytes. J. Clin. Invest. *108*, 871–878.

Marzo, A.L., Klonowski, K.D., Le Bon, A., Borrow, P., Tough, D.F., and Lefrançois, L. (2005). Initial T cell frequency dictates memory CD8+ T cell lineage commitment. Nat. Immunol. *6*, 793–799.

Masopust, D., Choo, D., Vezys, V., Wherry, E.J., Duraiswamy, J., Akondy, R., Wang, J., Casey, K.A., Barber, D.L., Kawamura, K.S., et al. (2010). Dynamic T cell migration program provides resident memory within intestinal epithelium. J. Exp. Med. *207*, 553–564.

Massberg, S., Schaerli, P., Knezevic-Maramica, I., Köllnberger, M., Tubo, N., Moseman, E.A., Huff, I.V., Junt, T., Wagers, A.J., Mazo, I.B., and von Andrian, U.H. (2007). Immunosurveillance by hematopoietic progenitor cells trafficking through blood, lymph, and peripheral tissues. Cell *131*, 994–1008.

Mueller, S.N., Gebhardt, T., Carbone, F.R., and Heath, W.R. (2013). Memory T cell subsets, migration patterns, and tissue residence. Annu. Rev. Immunol. *31*, 137–161.

Olson, J.A., McDonald-Hyman, C., Jameson, S.C., and Hamilton, S.E. (2013). Effector-like $CD8^+$ T cells in the memory population mediate potent protective immunity. Immunity *38*, 1250–1260.

Palframan, R.T., Jung, S., Cheng, G., Weninger, W., Luo, Y., Dorf, M., Littman, D.R., Rollins, B.J., Zweerink, H., Rot, A., and von Andrian, U.H. (2001). Inflammatory chemokine transport and presentation in HEV: a remote control mechanism for monocyte recruitment to lymph nodes in inflamed tissues. J. Exp. Med. *194*, 1361–1373.

Sallusto, F., Lenig, D., Förster, R., Lipp, M., and Lanzavecchia, A. (1999). Two subsets of memory T lymphocytes with distinct homing potentials and effector functions. Nature *401*, 708–712.

Sallusto, F., Geginat, J., and Lanzavecchia, A. (2004). Central memory and effector memory T cell subsets: function, generation, and maintenance. Annu. Rev. Immunol. *22*, 745–763.

Sarkar, S., Kalia, V., Haining, W.N., Konieczny, B.T., Subramaniam, S., and Ahmed, R. (2008). Functional and genomic profiling of effector CD8 T cell subsets with distinct memory fates. J. Exp. Med. *205*, 625–640.

Stary, G., Olive, A., Radovic-Moreno, A.F., Gondek, D., Alvarez, D., Basto, P.A., Perro, M., Vrbanac, V.D., Tager, A.M., Shi, J., et al. (2015). VACCINES. A mucosal vaccine against Chlamydia trachomatis generates two waves of protective memory T cells. Science *348*, aaa8205.

Steinert, E.M., Schenkel, J.M., Fraser, K.A., Beura, L.K., Manlove, L.S., Igyártó, B.Z., Southern, P.J., and Masopust, D. (2015). Quantifying Memory CD8 T Cells Reveals Regionalization of Immunosurveillance. Cell *161*, 737–749.

Voehringer, D., Blaser, C., Brawand, P., Raulet, D.H., Hanke, T., and Pircher, H. (2001). Viral infections induce abundant numbers of senescent CD8 T cells. J. Immunol. *167*, 4838–4843.

von Andrian, U.H., and Mackay, C.R. (2000). T-cell function and migration. Two sides of the same coin. N. Engl. J. Med. *343*, 1020–1034.

von Andrian, U.H., and Mempel, T.R. (2003). Homing and cellular traffic in lymph nodes. Nat. Rev. Immunol. *3*, 867–878.

Weninger, W., Crowley, M.A., Manjunath, N., and von Andrian, U.H. (2001). Migratory properties of naive, effector, and memory CD8(+) T cells. J. Exp. Med. *194*, 953–966.

Wherry, E.J., Teichgräber, V., Becker, T.C., Masopust, D., Kaech, S.M., Antia, R., von Andrian, U.H., and Ahmed, R. (2003). Lineage relationship and protective immunity of memory CD8 T cell subsets. Nat. Immunol. *4*, 225–234.

Williams, M.A., and Bevan, M.J. (2007). Effector and memory CTL differentiation. Annu. Rev. Immunol. *25*, 171–192.

Wright, D.E., Wagers, A.J., Gulati, A.P., Johnson, F.L., and Weissman, I.L. (2001). Physiological migration of hematopoietic stem and progenitor cells. Science *294*, 1933–1936.